Photochemistry and Photobiology, 2013, 89: 1417–1426

Photoreduction of Azaoxoisoaporphines by Amines: Laser Flash and Steady-State Photolysis and Pulse Radiolysis Studies†

Julio R. de la Fuente*[1], Christian Aliaga[1], Alvaro Cañete[2], Gabriel Kciuk[3], Tomasz Szreder[3] and Krzysztof Bobrowski[3]

[1]Departamento de Química Orgánica y Fisicoquímica, Facultad de Ciencias Químicas y Farmacéuticas, Universidad de Chile, Santiago, Chile
[2]Departamento de Química Orgánica, Facultad de Química, Pontificia Universidad Católica de Chile, Chile
[3]Institute of Nuclear Chemistry and Technology, Warsaw, Poland

Received 7 March 2013, accepted 22 April 2013, DOI: 10.1111/php.12087

ABSTRACT

Photoreduction of 7*H*-benzo[*e*]perimidin-7-one (3-AOIA, A1) and its 2-methyl derivative (2-Me-3-AOIA, A2) by non-H-donating amines (1,4-diazabicyclo[2.2.2]octane [DABCO]; 2,2,6,6-tetramethylpiperidine [TMP]), and a hydrogen-donating amine (triethylamine [TEA]), has been studied in deaerated neat acetonitrile solutions using laser flash photolysis (LFP) and steady-state photolysis. The triplet excited states of A1 and A2 were characterized by a strong absorption band with λ_{max} = 440 nm and lifetimes of 20 and 27 μs respectively. In the presence of tertiary amines, both triplet excited states were quenched with rate constants close to the diffusional limit (k_q ranged between 10^9 and 10^{10} M^{-1} s^{-1}). The transient absorption spectra observed after quenching with DABCO and TMP were characterized by maxima located at 460 nm and broad shoulders in the range of 500–600 nm. These transient species are attributed to solvent-separated radical ion pairs and/or to isolated radical anions. In the presence of TEA, these transients undergo proton transfer, leading to the neutral hydrogenated radicals, protonated over the N1- and O-atoms. Transient absorption spectra of these transients were characterized by maxima located at 400 and 520 nm and 430 nm respectively. Additional support for these spectral assignments was provided by pulse radiolysis (PR) experiments in acetonitrile and 2-propanol solutions.

INTRODUCTION

Oxoisoaporphines (OIA) alkaloids have been isolated from different families of plants such as *Menispermaceae* (1–3). These alkaloids that have been recognized as phototoxic phytoalexins, are synthesized by plants for the defense against pathogen agents or mechanical injuries (4–9). Due to the planar structure of the oxoisoaporphine derivatives, it is expected that these compounds might intercalate into DNA. Furthermore, because of the iminoquinone moiety in their structures, they could have redox activity that could interfere with mitochondrial electron transport (10,11). Derivatives have been tested as antiproliferative and antiplasmodial drugs, for malaria treatment. They show better selectivity against the *Plasmodium falciparum* parasite than does Chloroquine. They also have less toxicity to fibroblast than to the parasite (10,11). Recently, theoretical studies on the MAO-A inhibitory activity of some oxoisoaporphine derivatives, have been published, reporting that at least one derivative showed an IC_{50} value lower than MAO-A reference inhibitors (12). Moreover, some of them that contain two N atoms, for example, the 7*H*-benzo[*e*]perimidin-7-one derivatives, also called azaoxoisoaporphines (AOIA), have been synthesized as noncardiotoxic alternatives to anthraquinone antitumor drugs. They have also received considerable attention due to their antineoplastic and cytotoxic activity, *in vitro* and *in vivo*, toward multidrug resistant cell lines (13–19).

The relevant biological use of these molecules and the redox properties of their iminoquinone moiety make them a very interesting object of study including their radicals and radical ions generated in photochemical processes. Our earlier preliminary steady-state photolysis experiments of AOIA in acetonitrile, and in the presence of triethylamine (TEA) showed the appearance of absorption bands that were attributed to the hydrogenated anion (AH^-). When the photolyzed samples were either stored in the dark or exposed to O_2, the photoproducts reverted to the precursors and showed several isosbestic points (20). Surprisingly, the photolyzed samples stored in dark in the presence of D_2O showed a regioselective isotopic H/D exchange of protons at positions 4 and 6. A similar phenomenon has also been observed for the oxoisoaporphine derivatives (20). The ^{1}H-NMR study of the photoreduction of AOIA and OIA has provided the identity of the metastable photoproducts hydrogenated at the carbonyl O-atom (AOH^-). Their formation rationalizes the observed isotopic H/D exchange and supports the stepwise photoreduction mechanism elaborated earlier for 2,3-dihydro-oxoisoaporphines (2,3-dh-OIA) (21–23) and OIA (24).

The photoreduction mechanism proceeds through a stepwise electron-proton-electron transfer process (24). The first step is an excitation of the ground-state of 2,3-dh-OIA and OIA (A) to the excited singlet state (^{1}A) (Eq. 1), followed by an intersystem crossing to the lower energy excited triplet state (^{3}A) (Eq. 2). After a single photoinduced electron transfer from the amines to the excited triplet state of 2,3-dh-OIA and OIA (^{3}A) the radical ion pair complex is formed (Eq. 3). In the presence of non-H-donating amines; 1,4-diaza[2.2.2]-bicyclooctane (DABCO) and

*Corresponding author email: jrfuente@ciq.uchile.cl (Julio R. De la Fuente)
†This article is part of the Special Issue dedicated to the memory of Elsa Abuin.

2,2,6,6-tetramethylpiperidine (TMP), a back electron transfer leading to the respective substrates occurs (Eq. 4). On the other hand, in the presence of H-donating amines, such as TEA, the radical ion pair complex participates in a proton transfer reaction forming the neutral hydrogenated radical and an α-aminoalkyl radical (Eq. 5). A second electron transfer from the reductive α-aminoalkyl radical to the hydrogenated radical leads to the respective iminium cation and hydrogenated anion of the substrate (Eq. 6). The latter species is able to revert to the starting substrate either in the dark or by oxygen admission to the system. On the other hand, permanent products, for example aldehydes, secondary amines and diethylaminobutadiene, are formed from the iminium cation (Eq. 7) (21,22).

$$A + h\nu \rightarrow {}^1A \quad (1)$$

$${}^1A \rightarrow {}^3A \quad (2)$$

$${}^3A + R_2N - CH_2R' \rightarrow [A^{\bullet -} \bullet\bullet\bullet R_2N^{\bullet +} - CH_2R'] \quad (3)$$

$$[A^{\bullet -} \bullet\bullet\bullet R_2N^{\bullet +} - CH_2R'] \rightarrow A + R_2N - CH_2R' \quad (4)$$

$$[A^{\bullet -} \bullet\bullet\bullet R_2N^{\bullet +} - CH_2R'] \rightarrow [AH^{\bullet} \bullet\bullet\bullet R_2N - C^{\bullet}HR'] \rightarrow AH^{\bullet} + R_2N - C^{\bullet}HR' \quad (5)$$

$$[AH^{\bullet} \bullet\bullet\bullet R_2N - C^{\bullet}HR'] \rightarrow AH^{-} + R_2N^{+} = CHR' \quad (6)$$

$$R_2N^{+} = CHR' \rightarrow \text{Amine oxidation products} \quad (7)$$

The main difference between 3-AOIA currently studied and 2,3-dh-OIA and OIA studied previously, arises from the aromatic character of the ring containing the N-atom and from the presence of an additional N-atom at position 3 in the same aromatic ring respectively (Chart 1). It is expected that the additional N-atom changes the redox properties of the transient intermediates as well as the photophysical behavior compared to the previously studied derivatives.

Our studies include laser flash photolysis (LFP) experiments on 3-AOIA in the presence of amines: two non-H-donating amines (DABCO and TMP) and the hydrogen-donating amine (TEA). The first two were used for the spectral and kinetic characterization of the radical anions $A^{\bullet -}$ and/or radical ion pairs $[A^{\bullet -} \bullet\bullet\bullet R_2N^{\bullet +}\text{-}CH_2R']$. On the other hand, TEA was used for the identification of the hydrogenated radicals $AH^{\bullet}$. The identity of these intermediates was further confirmed by complementary pulse radiolysis (PR) experiments in acetonitrile and 2-propanol solutions in the absence of amines. Time-resolved studies were complemented by steady-state photolysis experiments that provided kinetic information on the proton transfer step that occurs during photoreduction of 3-AOIA in the presence of TEA.

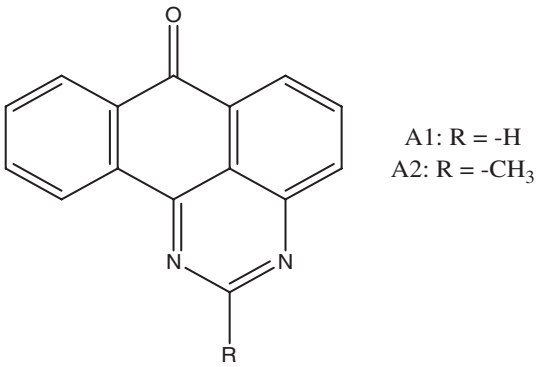

A1: R = -H
A2: R = -CH_3

Chart 1. 7H-benzo[e]perimidin-7-ones structures.

In this study, we have characterized the spectral and kinetic properties of transients formed in the photoreduction process of AOIA induced by amines. These studies provide a qualitative and partly quantitative picture of the reaction mechanism that was found to be dependent on the H-donating properties of the amines.

MATERIALS AND METHODS

Materials. Acetonitrile was purchased from Merck HPLC grade and used as received. TEA, 2,2,6,6-tetramethylpiperidine (TMP) and 1,4-diazabicyclo[2.2.2]octane (DABCO) were all purchased from Aldrich. The liquid amines were distilled in vacuum, trap to trap, sealed into glass tubes at 10^{-4} mm Hg. and stored at −18°C. Before each experiment, a new tube was opened to ensure the freshness of the amine. DABCO was used as received and its solutions were prepared immediately before use.

Synthesis of azaoxoisoaporphines. The synthesis of 7*H*-benzo[*e*] perimidin-7-one (3-azaoxoisoaporphine, 3-AOIA) and its methyl substituted derivative, 2-methyl-7*H*-benzo[*e*]perimidin-7-one (2-Me-3-azaoxoisoaporphine, 2-Me-3-AOIA) was performed by cyclization of 1-aminoantraquinone with N,N-dimethylformamide dimethyl acetal or N, N-dimethylacetamide-dimethyl-acetal with phosphorous oxychloride respectively. *In situ* cyclization of the intermediates formed was accomplished by an addition of ammonium acetate in hot ethanol (14,16,25).

Preparation of solutions. All solutions of AOIA for the LFP experiments were prepared with absorbance ≈0.6 at the excitation wavelength of 355 nm and concentration ≈0.1 mM. Solutions (3 mL) of AOIA in a 10 mm fluorescence quartz cell sealed with a septum were purged for 20 min. with Ar. Immediately after purging, an aliquot of either pure or diluted amine was added through the septum for the quenching or spectral experiments. For steady-state photolysis, AOIA absorbances were between 0.20 and 1.40 at 366 nm.

All solutions of AOIA (0.1 mM) for the PR experiments were prepared freshly before experiments in acetonitrile. Solutions were subsequently purged for at least 30 min. per 200 mL of sample with the desired gas before pulse irradiation (24,26,27).

Laser flash photolysis, LFP. Laser flash photolysis experiments were performed with a Q-switched Nd:YAG laser, Quantel Brilliant with the excitation at 355 nm. The flash photolysis setup was described previously (22,28,29).

Quenching of excited states. The lifetimes of the excited triplet states of AOIA, τ, were measured at different concentrations of quenchers at selected wavelengths. From the $1/\tau$ *vs* [quencher] plot, a modified Stern-Volmer equation $k_{obs} = k_0 + k_q[Q]$ was obtained, where $k_0 = 1/\tau^0$ is the decay rate constant for the excited triplet in absence of quencher; $k_{obs} = 1/\tau$ where τ is the lifetime in the presence of different concentrations of quencher [Q] and k_q is the bimolecular quenching rate constant.

Triplet energies. The triplet energies (E^T) of AOIA were estimated with the energy transfer method. The determination of the quenching constants with the selected energy acceptors (their triplet energies ranged between 255 and 146 kJ mol^{-1}) was performed by following the monoexponential decay of the triplets of AOIA at λ = 430 nm, using the modified Stern-Volmer equation (*vide supra*). The intersection point of two linear sections of the respective plot of the quenching rate constants (k_q) of the excited triplet state of AOIA *versus* the triplet energy (E^T) of the selected energy acceptors *(vide supra)* determines the triplet energy of the respective AOIA.

Generation of radical anions and hydrogenated radicals. The non-H-donating amines (TMP and DABCO) were used for spectral and kinetic characterization of the radical anions derived from AOIA ($A^{\bullet -}$) since the photoinduced electron transfer (PET) is not followed by proton transfer. On the other hand, the H-donating amine (TEA) was used for the spectral

and kinetic characterization of the hydrogenated radicals ($AH^{\bullet}$) since the PET is followed by proton transfer.

Pulse radiolysis, PR. Pulse radiolysis experiments were performed with the INCT LAE 10 linear accelerator with typical pulse lengths of 7–10 ns. The data acquisition system allows for kinetic traces to be displayed on multiple time scales. A detailed description of the experimental setup for optical measurements has been given elsewhere along with the basic details of the equipment and the data collection system (30,31). The irradiation cell was supplied with a fresh solution by a continuous and controlled flow. The dose per pulse, which was determined by thiocyanate dosimetry, was on the order of 18–20 Gy (1 Gy = 1 J kg^{-1}). Radiolytic yields are given in SI units as μmol J^{-1},that is the number of product species in micromoles that are generated for every joule of energy absorbed by the solution. All experiments were performed with a continuous flow of sample solutions at room temperature (~20°C). Experimental error limits are ±10% unless specifically noted.

Generation of radical ions. In Ar-saturated acetonitrile solutions containing AOIA, both, the radical anions and radical cations derived from them are generated by the reaction of solvated electrons or solvent radical anions and cations with a substrate (Eqs. 8–12). On the other hand, in O_2-saturated solutions only radical cations are formed (Eqs. 8 and 11) since the precursors of radical anions are scavenged by oxygen (Eq. 12) (32).

$$CH_3CN \rightsquigarrow CH_3CN^{\bullet+} + e^-_{solv} \quad (8)$$

$$e^-_{solv} + CH_3CN \rightarrow CH_3CN^{\bullet-} \quad (9)$$

$$e^-_{solv}/CH_3CN^{\bullet-} + A1/A2 \rightarrow A1^{\bullet-}/A2^{\bullet-} \quad (10)$$

$$CH_3CN^{\bullet+} + A1/A2 \rightarrow CH_3CN + A1^{\bullet+}/A2^{\bullet+} \quad (11)$$

$$e^-_{solv}/CH_3CN^{\bullet-} + O_2 \rightarrow O_2^{\bullet-} + CH_3CN \quad (12)$$

Generation of hydrogenated radical. In N_2O-saturated 2-propanol solutions containing AOIA, their neutral hydrogenated radicals are generated by a sequence of reactions displayed in equations (Eqs. 13–18).

$$(CH_3)_2CH - OH \rightsquigarrow (CH_3)_2CH{-}OH^{\bullet+} + e^-_{solv} \quad (13)$$

$$(CH_3)_2CH - OH^{\bullet+} + (CH_3)_2CH{-}OH \rightarrow (CH_3)_2C^{\bullet} - OH + (CH_3)_2CH{-}OH_2^{+} \quad (14)$$

$$e^-_{solv} + N_2O \rightarrow O^{\bullet-} + N_2 \quad (15)$$

$$O^{\bullet-} + (CH_3)_2CH - OH \rightarrow (CH_3)_2C^{\bullet}{-}OH + OH^- \quad (16)$$

$$(CH_3)_2C^{\bullet}{-}OH + A1/A2 \rightarrow (CH_3)_2C{=}O + A1^{\bullet-}/A2^{\bullet-} + H^+ \quad (17)$$

The radical anions $A1^{\bullet-}/A2^{\bullet-}$ formed in reaction (Eq. 17) undergo further protonation by protons formed in reactions (Eqs. 14 and 17) and/or by 2-propanol molecules (Eq. 18):

$$A1^{\bullet-}/A2^{\bullet-} + H^+/(CH_3)_2CH - OH_2^+/(CH_3)_2CH{-}OH \rightarrow A1H^{\bullet}/A2H^{\bullet} + (CH_3)_2CH - OH(CH_3)_2CH - O^- \quad (18)$$

Steady-state photolysis. The changes of absorbance with time were followed on an Agilent 8453 diode array spectrophotometer. The stirred solutions were photolyzed directly in the spectrophotometer cell holder with a 150 watts Black Ray UV lamp equipped with a 366 nm filter.

Photoconsumption quantum yields, (Φ_{pc}). A detailed description of the evaluation of photoconsumption quantum yields of AOIA has been given elsewhere (24). The variation in concentration of AOIA was evaluated from the absorbances measured at λ = 376 and 380 nm for 3-AOIA and 2-Me-3-AOIA respectively (24). The photon flux was determined by using Aberchrome®540 (33).

RESULTS AND DISCUSSION

Steady-state photolysis. UV–Vis spectroscopy

Photoreduction of AOIA A1 and A2 by H-donating amines such as TEA, is an efficient process in deoxygenated solutions of different solvents. An occurrence of a clean photoreaction leading to the azaoxoisoaporphine hydrogenated anions is indicated by the evolution of spectra revealing several isosbestic points. A similar behavior was observed in several solvents such as acetonitrile, methanol, benzene and cyclohexane (Fig. 1) (20).

The small differences in behavior are due to the absorption band structure of photoproducts at longer wavelengths and slight changes in the position of isosbestic points during photolysis. From the photoreduction with TEA in acetonitrile, the molar absorption coefficients (ε) of the photoproducts (ε_{450} = 5530 and ε_{470} = 6240 M^{-1} cm^{-1} for $A1OH^-$ and $A2OH^-$ respectively) were estimated by using the ratios of the absorbances at absorption maxima of the photoproducts and the parent AOIA bands. In all of the mentioned solvents the photoproducts revert back to the initial AOIA when the samples are stored in the dark or faster if air was admitted into the reaction mixture.

The photoconsumption quantum yields, Φ_{pc}, showed a strong dependency on the amine concentration, reaching a limiting value $\Phi_{pc} \approx 1$ at molar concentration ratios [TEA]/[AOIA] > 300 and

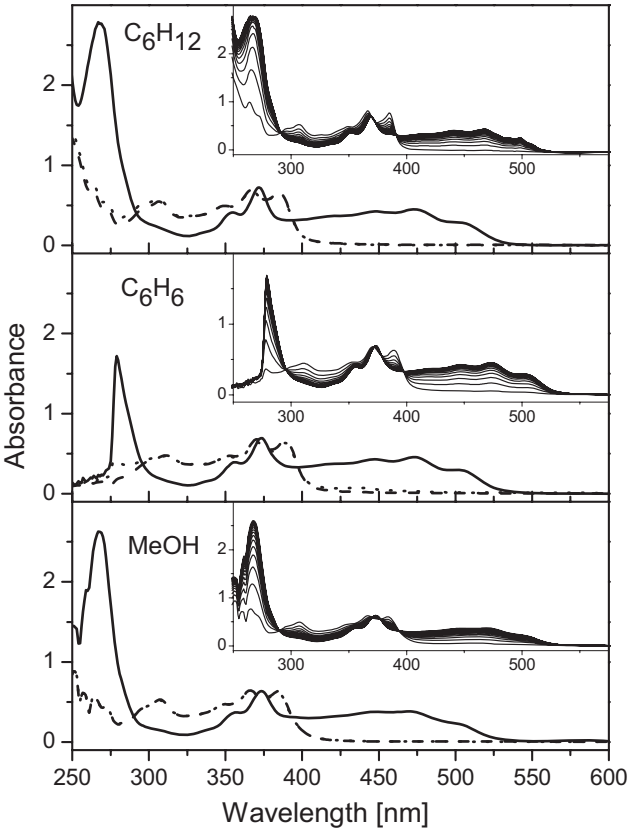

Figure 1. Absorption spectra recorded at the beginning (dashed line), at the end of photolysis (solid line) and with an access of air after photolysis (dotted line) for A2/TEA system in (a) cyclohexane, (b) benzene and (c) methanol. Insets: Evolution of absorption spectra recorded during photolysis in the respective solvents. The sharp break below 275 nm in benzene is due to solvent absorption.

>10 for A1 and A2 respectively (Fig. 2). Similar behavior was observed in all solvents used, that is in cyclohexane, benzene and methanol.

For A1, irrespective of the solvent used, Φ_{pc} was nearly 1. However, for A2, Φ_{pc} increases with the solvent polarity from 0.74 in cyclohexane to 0.97 in acetonitrile and 0.91 in methanol showing that Φ_{pc} can be roughly related to the solvent polarity. Values of Φ_{pc} for A1 and A2 together with the empirical parameter for solvent polarity (E_T) (34) are summarized in Table 1.

Assuming the earlier proposed photoreduction mechanism for 2,3-dh-OIA and OIA (Eqs. 1–7), one can derive Eq. (19) that relates Φ_{pc} with amine concentration:

$$\Phi_{pc} = \frac{\Phi^T k_{H^+} k_{ET}[\text{amine}]}{(k_{-ET} + k_{H^+})(k_0 + k_{ET}[\text{amine}])} \qquad (19)$$

where Φ^T is the triplet quantum yield, k_0 is the deactivation kinetic constant of the excited triplet state, k_{ET} is the rate constant for the photoinduced electron transfer, k_{-ET} is the rate constant for the back electron transfer and k_{H+} is the rate constant for the proton transfer. Rearranging Eq. (19) to a linear relationship between $1/\Phi_{pc}$ and 1/[amine] represented by Eq. (20), one can easily extract the value of the intercept/slope ratio equal to $k_{ET} \times \tau^0$. The parameter $\tau^0 = 1/k_0$ represents the excited triplet state lifetime in the absence of amine.

$$\frac{1}{\Phi_{pc}} = \frac{(k_{-ET}+k_{H^+})}{\Phi^T k_{H^+}}\left[1+\frac{1}{k_{ET}\tau^0}\times\frac{1}{[\text{amine}]}\right] \qquad (20)$$

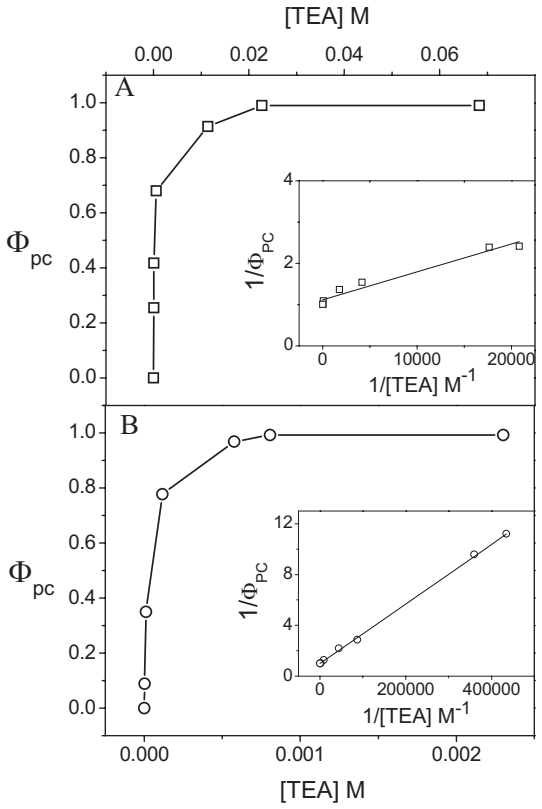

Figure 2. The dependence of photoconsumption quantum yields, Φ_{pc} on [TEA] in acetonitrile for (A) 100 μM A1 (□) and (B) 80 μM A2 (○). Insets: Plots of $1/\Phi_{pc}$ *vs* 1/[amine] according to Eq. (20).

Table 1. Photoconsumption quantum yields, Φ_{pc}, for azaoxoisoaporphines A1 and A2, in the presence of TEA (see text for details).

	Φ_{pc}	
Solvent (E^N_T)*	A1	A2
Methanol (0.762)	0.97 ± 0.03	0.91 ± 0.01
Acetonitrile (0.460)	0.98 ± 0.02	0.97 ± 0.03
Benzene (0.111)	0.99 ± 0.01	0.82 ± 0.01
Cyclohexane (0.006)	0.99 ± 0.01	0.74 ± 0.02

*Empirical parameter for solvent polarity E^N_T (34).

Taking the values of the intercepts from the plots (insets in Fig. 2) together with $\Phi^T = 1$ (*vide infra*), it was possible to calculate the ratio of proton transfer and back electron transfer rate constants (k_{H+}/k_{-ET}). These processes account for the decomposition of the radical anions in the ion pairs formed after the photoinduced electron transfer. The ratios of 6.3 and 33 were calculated for A1/TEA and A2/TEA respectively. These values were affected by large uncertainties. However, they indicate that the proton transfer from the amine radical cation to the radical anion of A1 and A2 in an ion pair was faster than the back electron transfer. Since the decay rates of the radical anions $A1^{\bullet -}$/$A2^{\bullet -}$ or radical ion pairs [$A1^{\bullet -}$/$A2^{\bullet -}$ ••• $Amine^{\bullet +}$] measured in the presence of DABCO were similar for A1 and A2 (*vide infra*), it is reasonable to assume that the back electron rate constants (k_{-ET}) are similar for A1 and A2. Taking this assumption into account, one can easily calculate that the proton transfer rate constant (k_{H+}) for A2 is approximately five-fold larger than for A1. This difference in the kinetic behavior could be due to a greater reactivity of the radical anion $A2^{\bullet -}$, induced by the methyl group located at position 2 on the molecule.

Laser flash photolysis and pulse radiolysis

Excited triplet states (^{3}A1 and ^{3}A2): generation and spectral/kinetic characterization. After the light absorption, the excited singlet states (^{1}A1 and ^{1}A2) were formed which further undergo an efficient intersystem crossing to the lower energy excited triplet states (^{3}A1 and ^{3}A2) with the quantum yield close to unity, see Table 1 (35,36). For both compounds the absorption spectra of triplets were characterized by intense absorption bands with maxima located at λ = 440–450 nm and a shoulder at ~410 nm. They also showed depletion in their ground absorptions below 370 nm (Fig. 3).

These transients (^{3}A1 and ^{3}A2) decayed mono-exponentially with lifetimes of τ = 20 and 27 μs respectively. Their absorption spectra disappeared completely in O_2-saturated solutions confirming their assignment as the excited triplet states. The excited triplets (^{3}A1 and ^{3}A2) were subsequently quenched by triplet energy acceptors with known triplet energies (E^T). From this information, estimations of their triplet energies were made. (37) A typical Stern-Volmer plot for ^{3}A2 quenching by perylene is presented in the inset in Fig. 4. All quenching rate constants measured are summarized in Table 2. From the plot of the quenching rate constants *vs* the triplet energy of the acceptors, the triplet energies (E^T = 182 and 181 kJ mol^{-1} for ^{3}A1 and ^{3}A2 respectively) were estimated (Fig. 4).

The E^T values of ^{3}A1 and ^{3}A2 were found to be more than 10 kJ mol^{-1} less than the E^T values measured for triplet states derived from OIA (24). The stabilization of ^{3}A1 and ^{3}A2 with respect to the triplet states of oxoisoaporphines (^{3}OIA) can be

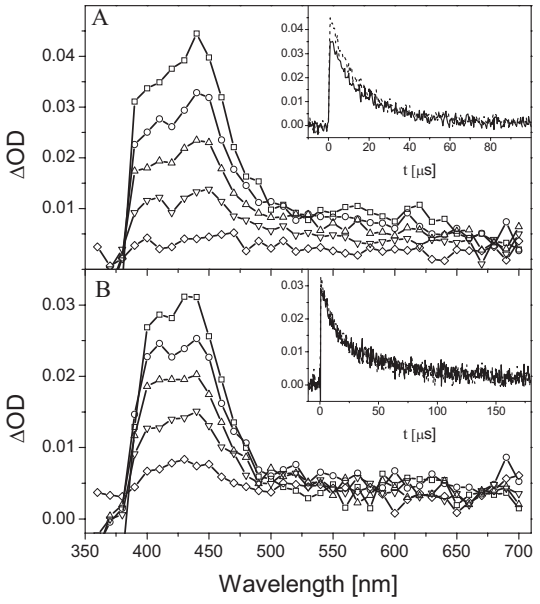

Figure 3. Triplet–triplet transient absorption spectra recorded after 1 (□), 5 (○), 10 (△), 20 (▽) and 50 μs (◊) after the laser pulse in acetonitrile solutions containing 80 μM of A1 (A) and A2 (B). Insets: Kinetic time profile representing decays of ^{3}A1* and ^{3}A2* at λ = 410 (solid line) and λ = 440 nm (dashed line).

Table 2. Quenching rate constants (k_q), for A1 and A2 with the selected quenchers, and its triplet state energies.

Quencher	Triplet energy† [kJ mol^{-1}]	k_q [M^{-1} s^{-1}]	
		^{3}A1	^{3}A2
Perylene*	146	$(5.2 \pm 0.1) \times 10^{10}$	$(4.5 \pm 0.1) \times 10^{10}$
Azulene*	163	$(1.9 \pm 0.1) \times 10^{10}$	$(1.6 \pm 0.1) \times 10^{10}$
Rhodamine-6G	180	$(8.4 \pm 0.3) \times 10^{9}$	$(6.3 \pm 0.4) \times 10^{9}$
Acridine orange	205	$(9.4 \pm 0.4) \times 10^{8}$	$(7.5 \pm 0.2) \times 10^{8}$
Naphthalene*	253	$(8.0 \pm 0.2) \times 10^{7}$	$(7.7 \pm 0.3) \times 10^{7}$
Quinoxaline*	255	$(4.9 \pm 0.1) \times 10^{7}$	$(6.2 \pm 0.3) \times 10^{7}$
E^T [kJ mol^{-1}]	—	182 ± 4	181 ± 4

*Quencher solutions were prepared in benzene. Aliquots of these solutions were added to A1/A2 solutions in acetonitrile. †Data taken from (37).

attributed to the presence of the second N-atom in the AOIA molecules.

Radical anions (A1$^{\bullet-}$ and A2$^{\bullet-}$): generation and spectral/kinetic characterization. The excited triplets (^{3}A1 and ^{3}A2) were also efficiently quenched by amines such as TMP or DABCO with quenching rate constants close to the diffusion limit (Table 3). Since these amines are not able to donate H-atoms, the photoreactions proceed only to the formation of the radical ion pair (by an analogous reaction to that described by Eq. 3) that would revert to the ground states of substrates by a back electron transfer (analogous to the reaction described by Eq. 4). Therefore, in the presence of these amines it is possible to characterize the kinetic and spectroscopic properties of the radical anions/radical ion pairs derived from the respective AOIA. Neither TMP nor DABCO produce any photoproduct in a steady-state photolysis.

The k_{ET} increase of the ET process involving ^{3}A1/^{3}A2 and TMP in comparison to the k_{ET} of analogous process involving

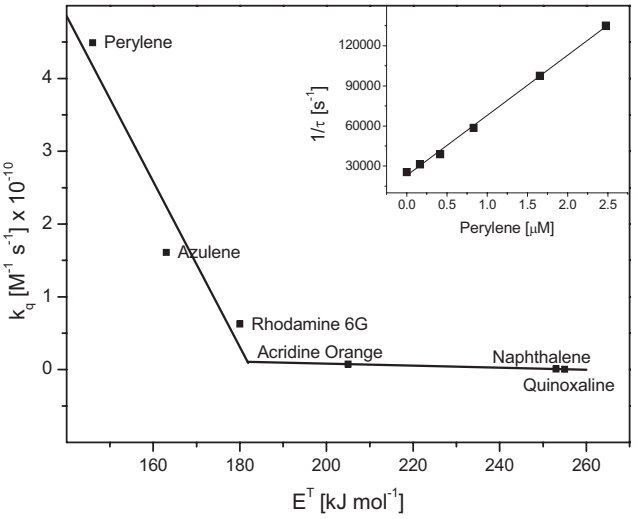

Figure 4. Plot of the quenching rate constants of the excited triplet state of (^{3}A2) *versus* the triplet energy (E^T) of several energy acceptors. Inset: Representative plot for the quenching of ^{3}A2 by perylene according to a modified Stern-Volmer equation (vide supra subchapter: Quenching of excited states). For all quenchers linear behavior of Stern-Volmer plots was observed ($r > 0.99$).

^{3}OIAs can be rationalized in terms of the greater reduction potentials of ^{3}A1/^{3}A2 caused by the presence of the second electronegative N-atom in the A1/A2 molecules.

By using sufficiently high concentrations of amines (DABCO or TMP) to rapidly quench almost all of the AOIA triplets (^{3}A1 and ^{3}A2), new absorption bands appeared, which were attributed either to the radical anions A1$^{\bullet-}$/A2$^{\bullet-}$ or to the radical ion pairs involving the respective radical cations of the amines [A1$^{\bullet-}$/A2$^{\bullet-}$ ••• Amine$^{\bullet+}$]. For both AOIA strong absorption bands were observed, with the maxima located at λ = 460 nm and shoulders at λ = 400 nm and less intense broad bands located between 500 and 600 nm (Fig. 5). The features of the absorption spectra obtained were independent of the amine used.

However, their lifetimes strongly depended on the nature of the electron donor. With DABCO used as a quencher, the lifetimes of transients derived from A1/A2 (*vide supra*) were close to τ = 20 μs. Similar lifetimes of transients derived from oxoisoaporphines (OIA and 5-MeO-OIA) were measured (24). Interestingly, with TMP used as a quencher, the lifetimes of the transients substantially increased, to nearly τ = 1 ms. This observation suggests the formation of a long-lived contact radical ion pair, CRIP, [A1$^{\bullet-}$/A2$^{\bullet-}$ ••• TMP$^{\bullet+}$], which is likely stabilized by a hydrogen bond involving the amine hydrogen of TMP. Similar phenomena were also observed for transients derived from OIA where the lifetimes of the respective transients derived from OIA, A3 and 5-MeO-OIA, A4, were found as τ = 140 μs and 0.9 ms respectively (24).

Radical anions (A1$^{\bullet-}$ and A2$^{\bullet-}$) generation by pulse radiolysis. Pulse radiolysis of acetonitrile solutions containing A1 and A2 was performed in order to resolve whether the absorption spectra generated by the LFP in the presence of DABCO and TMP can be assigned to radical anions (A1$^{\bullet-}$/A2$^{\bullet-}$) or to the respective ion-radical pairs [A1$^{\bullet-}$/A2$^{\bullet-}$ ••• TMP$^{\bullet+}$].

Azaoxoisoaporphines A1 and A2 exhibit similar behavior under PR. In Ar-saturated acetonitrile solutions containing A1,

Table 3. Quenching rate constants of the excited triplet states (^{3}A) derived from azaoxoisoaporphines (A1 and A2) and oxoisoaporphines (OIA, A4; and 5-MeO-OIA, A5) by selected amines, in acetonitrile.

Amine (E^0 [V] *vs* NHE)	k_{ET} [M^{-1} s^{-1}]			
	^{3}A1	^{3}A2	^{3}A4*	^{3}A5*
TMP (1.36)	$(1.2 \pm 0.1) \times 10^9$	$(1.1 \pm 0.1) \times 10^9$	$(8.9 \pm 0.2) \times 10^6$	$(9.6 \pm 0.2) \times 10^6$
DABCO (0.84)	$(1.0 \pm 0.1) \times 10^{10}$	$(1.0 \pm 0.2) \times 10^{10}$	$(3.8 \pm 0.3) \times 10^9$	$(3.2 \pm 0.2) \times 10^9$
TEA (1.02)	†	†	$(1.1 \pm 0.1) \times 10^9$	$(1.2 \pm 0.1) \times 10^9$

*Data taken from (24). †Spectral overlapping prevents the determination of k_{ET}.

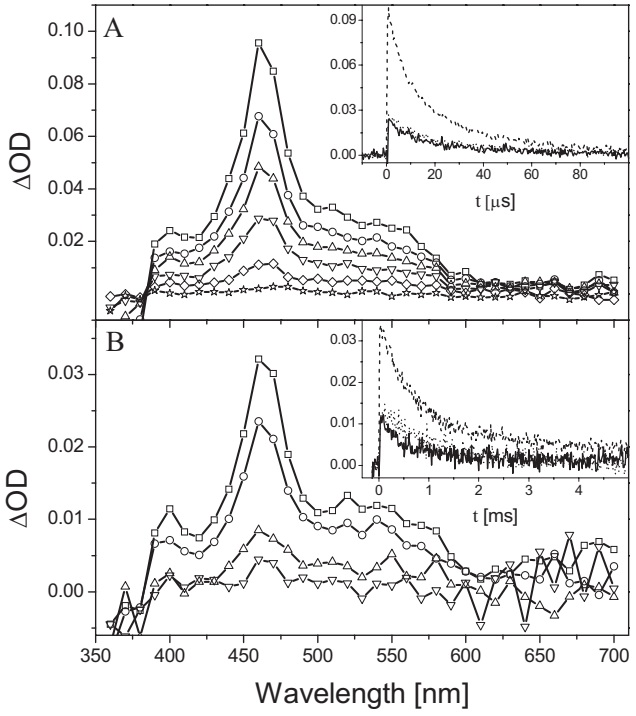

Figure 5. Absorption spectra recorded in Ar-saturated acetonitrile solutions containing 80 μM A1 in presence of: (A) 1 mM DABCO at 1 (□), 5 (○), 10 (△), 20 (▽), 50 (◊) and 150 μs (☆) after laser pulse; (B) 1.4 mM TMP at 20 μs (□), 100 μs (○), 500 μs (△) and 1 ms (▽) after laser pulse. Insets: the kinetic long time profiles representing decays of absorbance at λ = 400 nm (solid line), 460 nm (dashed line) and 540 nm (dotted line).

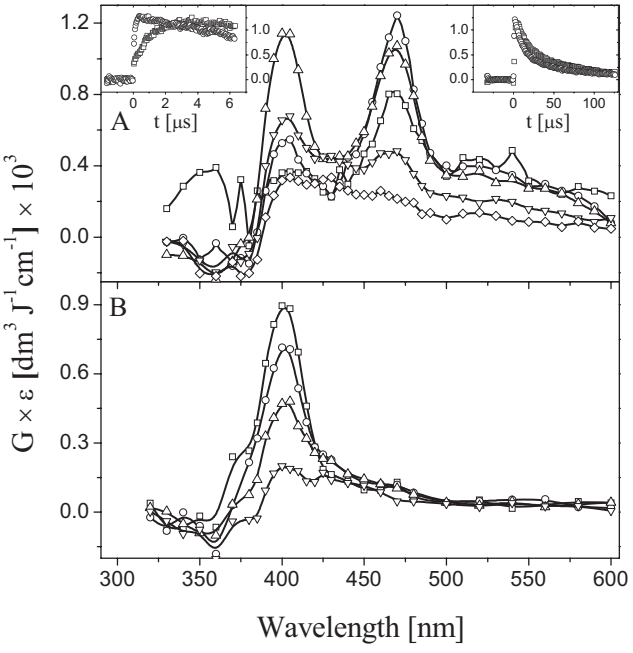

Figure 6. (A) Transient absorption spectra observed at 0.05 μs (□), 0.32 μs (○), 3.2 μs (△), 20 μs (▽) and 60 μs (◊) after pulse irradiation of an Ar-saturated acetonitrile solution containing 0.1 mM A1; (B) at 3.2 μs (□), 10 μs (○), 20 μs (△) and 60 μs (▽) after pulse irradiation of an O_2-saturated acetonitrile solution for the same substrate. Insets: Kinetic time profiles representing formation and decays of the absorption bands at λ = 400 nm (□) and 470 nm (○).

the absorption spectra recorded in the sub-microsecond time domain were characterized by two strong absorption bands with maxima located at λ = 400–405 nm and λ = 470 nm with a pronounced shoulder in the spectral range from 510 to 600 nm which are attributed to the radical cations ($A1^{\bullet+}$) and radical anions ($A1^{\bullet-}$) respectively (Fig. 6A). In O_2-saturated acetonitrile the absorption spectra recorded in the same time domain were characterized only by a distinct absorption band with maximum located at λ = 400–405 nm. This absorption band is assigned to the radical cations ($A1^{\bullet+}$) (Fig. 6B).

Kinetic time profiles were recorded at the absorption maxima of $A1^{\bullet+}$ (λ_{max} = 400 nm) and $A1^{\bullet-}$ (λ_{max} = 470 nm). These profiles clearly showed that the formation of $A1^{\bullet-}$ was faster than the formation of $A1^{\bullet+}$. The first-order fittings of these kinetic time profiles gave the pseudo-first-order rate constants $k = 9.3 \times 10^6$ s^{-1} and $k = 9.9 \times 10^5$ s^{-1} for the formation of $A1^{\bullet-}$ and $A1^{\bullet+}$, respectively, at 0.1 mM concentration of A1. The same fitting procedure performed for A2 gave the pseudo-first-order rate constants $k = 8.2 \times 10^6$ s^{-1} and $k = 7.3 \times 10^5$ s^{-1} of the formation of $A2^{\bullet-}$ and $A2^{\bullet+}$, respectively, at 0.1 mM concentration of A2 (data not shown).

To extract the spectra of radical anions one has to subtract the absorption spectra obtained in O_2-saturated solutions from the respective absorption spectra obtained in Ar-saturated solutions. This approach was successfully applied earlier for 2,3-dihydro-oxoisoaporphines (26) and OIA (24).

The absorption spectra of $A1^{\bullet-}$ (data not shown) and $A2^{\bullet-}$ (Fig. 7A), exhibit a distinct, intense absorption band with a maximum located at λ = 470 nm and a broad band in the spectral range from 500 to 600 nm. These spectra are very similar in shape and spectral features to the spectra generated photochemically in acetonitrile solutions containing A1 and A2 in the presence of DABCO (Fig. 7B) and TMP. The absorptions decay mono-exponentially at both wavelengths with lifetimes (τ) of 20 and 11 μs for $A1^{\bullet-}$ and $A2^{\bullet-}$ respectively (Fig. 7A, inset). These kinetic parameters are very similar to those observed for absorptions generated photochemically in the presence of DABCO (Fig. 7B, inset).

Neutral hydrogenated radicals (A1H$^{\bullet}$ and A2H$^{\bullet}$): generation and spectral/kinetic characterization. Neutral hydrogenated radicals (A1H$^{\bullet}$ and A2H$^{\bullet}$) were generated in acetonitrile solutions by the photoreduction of the respective AOIA in the presence of the H-donating amine, TEA. The transient absorption spectra recorded at $t > 10$ μs were characterized by a distinct absorption band with $\lambda_{max} = 460$ nm and several less intense bands with weakly pronounced absorption maxima located at $\lambda = 400$, 510 and 550 nm for A1 (Fig. 8A) and $\lambda = 410$, 520 and 580 nm for A2 (Fig. 8B). In the case of A2, after a long time decay (0.9 ms) the absorption band at $\lambda = 460$ nm was substantially quenched in comparison to the still dominant 460 nm-band for A1.

By analogy to the spectral features observed with DABCO and TMP, the absorption band with $\lambda_{max} = 460$ nm can be attributed to the long-lived contact radical ion pairs [A1$^{\bullet-}$/A2$^{\bullet-}$ ••• TEA$^{\bullet+}$], which decay with lifetimes $\tau = 362$ μs and 127 μs for A1 and A2 respectively. These lifetimes were shorter than those observed in the presence of TMP, but they were much longer than those measured in the presence of DABCO or by PR. These observations strongly suggest the formation of a CRIP in the presence of TEA.

The remaining absorption bands, located at 400, 510 and 550 nm for A1 and at 410, 430, 520 and 580 nm for A2, grew very rapidly, with similar first-order kinetics. However, due to the large contribution of the radical anions at these wavelengths, it was not possible to resolve the kinetic behavior involving the radical anions and hydrogenated radicals at short time delays. However, from the decay kinetics of A1$^{\bullet-}$/A2$^{\bullet-}$ or [A1$^{\bullet-}$/A2$^{\bullet-}$ ••• TEA$^{\bullet+}$], with lifetimes $\tau = 362$ μs and 127 μs, respectively, and assuming that their decays occurred mostly by protonation, one can estimate the ratio $k_{H+}(A2)/k_{H+}(A1)$ ~2.8. This value agrees fairly well with the value estimated from the steady-state photolysis (*vide supra*).

Furthermore, the less intense absorptions at 400, 510 and 550 nm (for A1H$^{\bullet}$) and those at 410, 520 and 580 nm (for A2H$^{\bullet}$) decayed uniformly with $\tau = 270$ and 97 μs respectively. On the other hand, the absorption at 430 nm (for A2H$^{\bullet}$) decayed with $\tau = 115$ μs. These decays with distinct lifetimes for A2H$^{\bullet}$ strongly suggest the presence of at least two kinds of protonated radicals A2H$^{\bullet}$. The same behavior was also observed for aromatic OIA (24). Therefore, this behavior cannot be disregarded for A1H$^{\bullet}$. Unfortunately, due to the strong overlap of absorption bands of hydrogenated radicals (A1H$^{\bullet}$) and the respective radical ions (A1$^{\bullet-}$) or radical ion pairs [A1$^{\bullet-}$ ••• TEA$^{\bullet+}$], it was not possible to resolve their decay kinetics.

Neutral hydrogenated radicals (A1H$^{\bullet}$ and A2H$^{\bullet}$) generated by pulse radiolysis. Pulse radiolysis of 2-propanol solutions containing A1 and A2 was carried out in order to confirm the assignments of the absorption bands generated by the LFP in the presence of TEA to neutral hydrogenated radicals (A1H$^{\bullet}$/A2H$^{\bullet}$).

Azaoxoisoaporphines A1 and A2 exhibit similar behavior under PR. In N_2O-saturated 2-propanol solutions containing 0.1 mM A1/A2, the absorption spectra were fully developed at 40 μs after the electron pulse. They were characterized by three distinct

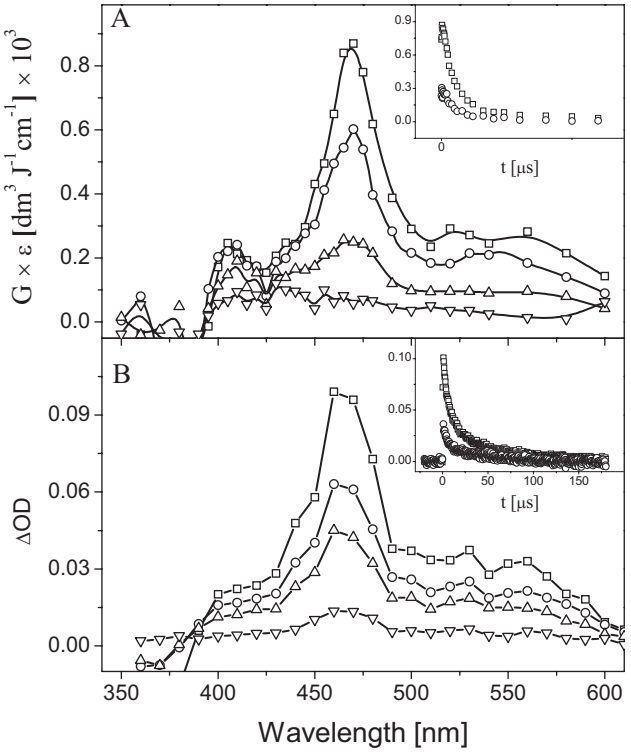

Figure 7. (A) Corrected absorption spectra (see explanation in the text) recorded in acetonitrile solution containing 0.1 mM A2 at 0.6 (□), 4.8 (○), 16 (▽) and 60 μs (▽) after pulse irradiation. Inset: Decay kinetics of A2$^{\bullet-}$ recorded at 470 (□) and 560 nm (○). (B) Absorption spectra recorded in Ar-saturated acetonitrile solutions containing 80 μM A2 in presence of 22 mM DABCO at 1 μs (□), 5 μs (○), 10 μs (△) and 50 μs (▽) after the laser pulse. Inset: Decay kinetics recorded at 460 (□) and 560 nm (○).

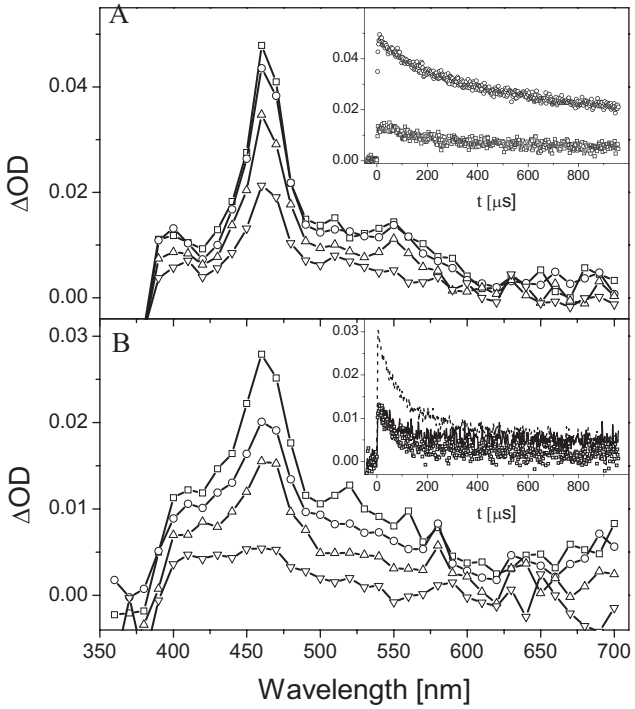

Figure 8. Absorption spectra in Ar-saturated acetonitrile containing 40 mM TEA and (A) 65 μM A1 and (B) 80 μM A2 recorded at 10 μs (□), 50 μs (○), 200/100 μs (△) and 900 μs (▽) after laser pulse. Inset in A: decay kinetics recorded at $\lambda = 400$ nm (□) and 460 nm (○). The decay kinetics recorded at $\lambda > 500$ nm overlap with the decay kinetics at $\lambda = 400$ nm (data not shown). Inset in B: decay kinetics recorded at $\lambda = 410$ nm (solid line), 460 nm (dashed line) and 520 nm (□).

absorption bands with maxima located at $\lambda = 400$, 430 and 520 nm (Fig. 9A and B). Absorptions recorded at these wavelengths grow in exponentially with an average pseudo-first-order rate constant $k = 1.3 \times 10^5\ s^{-1}$ for A1 and $k = 3.0 \times 10^5\ s^{-1}$ for A2. Taking into account the sequence of reactions (Eqs. 13–18) and on the basis of our earlier LFP observations (*vide supra*), these absorptions can be tentatively assigned to the neutral hydrogenated radicals (A1H$^\bullet$/A2H$^\bullet$). Interestingly, absorptions recorded at $\lambda = 400$ and 520 nm for both AOIA A1 and A2 decay faster ($k = 2.9 \times 10^3\ s^{-1}$ and $3.8 \times 10^3\ s^{-1}$ respectively) compared with absorption recorded at $\lambda = 430$ nm ($k = 2.1 \times 10^3\ s^{-1}$ and $3.0 \times 10^3\ s^{-1}$ respectively). These observations would account for the existence of two types of hydrogenated radicals with protonation sites located on the oxygen atom (A1OH$^\bullet$/A2OH$^\bullet$) and the nitrogen atom (A1N1H$^\bullet$/A2N1H$^\bullet$). Based on thermodynamic stabilities and the observed isotope exchange (20) the species absorbing at $\lambda = 430$ nm with the lifetimes $\tau = 470$ and 330 μs can be identified as A1OH$^\bullet$ and A2OH$^\bullet$ respectively. The remaining absorption bands with maxima at $\lambda = 400$ and 520 nm are assigned to the neutral hydrogenated radicals A1N1H$^\bullet$/A2N1H$^\bullet$. Their respective lifetimes $\tau = 370$ and 260 μs, shorter than those for A1OH$^\bullet$/A2OH$^\bullet$, confirm their lower thermodynamic stability.

By considering formation enthalpies for AN1H$^\bullet$ and AOH$^\bullet$ radicals, with a $\Delta\Delta H_f^\circ$ defined as ($\Delta H_f^\circ{}_{AN1H^\bullet} - \Delta H_f^\circ{}_{AOH^\bullet}$) of 3.23 and 3.01 kcal mol^{-1} for A1 and A2, respectively (20), one can expect that both radicals are present in an equilibrium, likely mediated by the excess of amine as postulated earlier for OIA (24).

DISCUSSION

This work reports for the first time the spectral and kinetic data regarding the triplets, radical anions/radical ion pairs and neutral hydrogenated radicals derived from two AOIA, that is 7*H*-benzo[*e*]perimidin-7-one (3-AOIA, A1) and its 2-methyl derivative (2-Me-3-AOIA, A2). In addition, application of PR (as a complementary method for the generation of radical ions) was used to generate selectively and to observe the radical anions of A1 and A2 in absence of amines.

For both compounds the absorption spectra of triplets were characterized by intense absorption bands with maxima located at $\lambda = 440$–450 nm and a shoulder at ~410 nm, and depletions of the ground absorption below 370 nm (Fig. 3). Triplet energies E^T of 182 and 181 kJ mol^{-1}, were estimated, for ^{3}A1 and ^{3}A2 respectively. These energies are nearly 10 kJ mol^{-1} lower than those reported for OIA (24). This stabilization can be attributed to the presence of the second electronegative N-atom in the AOIA structure. The presence of the second N-atom does not affect the triplet quantum yield, Φ^T, as compared with the OIA, (24) but these newly measured triplet quantum yields are significantly larger than those measured for 2,3-dihydro-oxoisoaporphines derivatives, which were 0.38; 0.42 and 0.55 for the 5,6-dimethoxy; 5-methoxy and the unsubstituted one respectively (22,23). However, this second N-atom, substantially affects the photoconsumption quantum yields, Φ_{pc}. The value $\Phi_{pc} = 1$ is significantly larger than $\Phi_{pc} = 0.25$ and 0.41 measured earlier for OIA and 5-MeO-OIA respectively (24). These photoconsumption quantum yields were all around 0.1 for the 2,3-dh-OIA derivatives (23). Therefore, the aromatic character of the OIA increases the triplet quantum yields and the N-atom in the AOIA, increases the photoconsumption by affecting the rate of the proton transfer step in the radical ion pair $A^{\bullet-}$ ••• $R_2N^{\bullet+}$-CH_2R'.

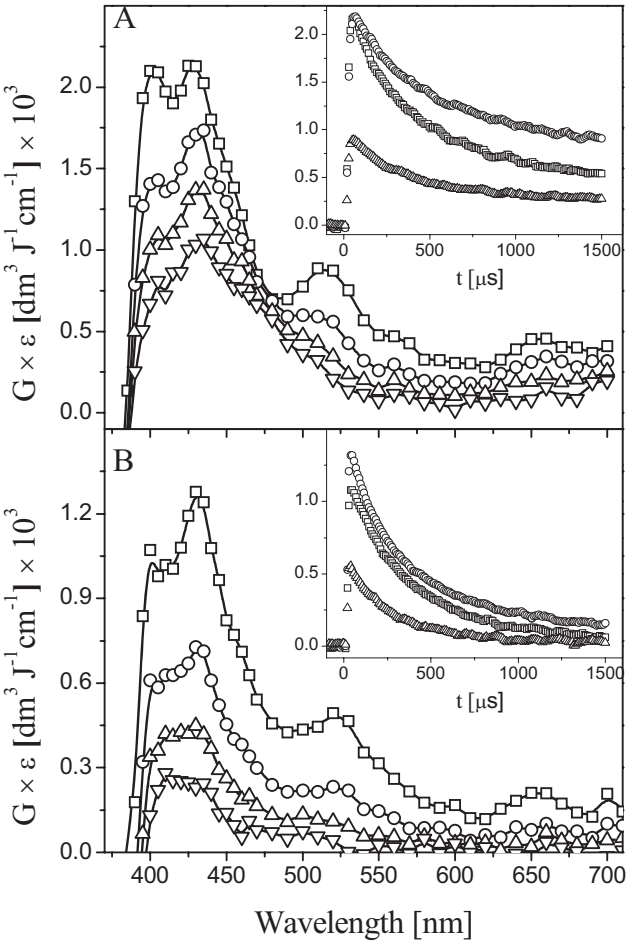

Figure 9. Transient absorption spectra recorded at 40 μs (□), 240 μs (○), 500 μs (△) and 1000 μs (▽) after pulse irradiation of an N_2O-saturated 2-propanol solutions containing: (A) 0.1 mM A1 and (B) 0.1 mM A2. Insets: decay kinetics recorded at $\lambda = 400$ nm (□), 430 nm (○) and 520 nm (△).

The absorption spectra of radical anions or radical ion pairs, $A^{\bullet-}$or [$A^{\bullet-}$ ••• $R_2N^{\bullet+}$-CH_2R'], generated photochemically for A1 and A2 in the presence of non H-donating amines do not differ substantially from those generated by PR. However, the lifetimes of those generated photochemically in the presence of TMP are much longer than those generated by PR. This observation reveals a strong interaction between A1$^{\bullet-}$/A2$^{\bullet-}$ with TMP$^{\bullet+}$, in a form of CRIP. Such a strong interaction in the radical ion pair can be understood by considering an H-bond between the NH from the radical cation of TMP and the radical anion of the substrate (38). However, even with this interaction the absorption spectra for the radical anions A1$^{\bullet-}$ or A2$^{\bullet-}$ are nearly identical to those obtained in the presence of DABCO and those generated by PR.

A similar behavior was observed with TEA where the CRIP prevails at longer times after the laser pulse. Again, this interaction does not considerably affect the spectra of the radical anions, which appear to be the dominant species together with the hydrogenated radicals. In spite of the fact that the substantial overlapping of the absorption spectra of the ion-radical pairs ([$A^{\bullet-}$ ••• $TEA^{\bullet+}$]) and hydrogenated radicals (AH$^\bullet$), which precludes their unequivocal kinetic characterization, it is clear that two distinct AH$^\bullet$ radicals are formed. On the basis of the PR

results in 2-propanol solutions and the thermodynamic data (20), we can tentatively assign the absorption bands at 400 and 520 nm to the AN1H$^{\bullet}$ radicals and the other bands at 430 nm to the AOH$^{\bullet}$ radicals. These radicals probably exist in equilibrium, as it was postulated earlier for oxoisoaporphine derivatives (24).

It is interesting to note that the characteristic band assigned to the radical anions/radical ion pairs (A1$^{\bullet-}$/[A1$^{\bullet-}$ ••• TEA$^{\bullet+}$]) is observed at very long times (900 μs) after the laser pulse while that for A2$^{\bullet-}$ nearly disappeared. This observation is in line with the fact that the proton transfer proceeds 2.9–5-fold faster for A2$^{\bullet-}$ than for A1$^{\bullet-}$. Thus, one can conclude that the absorption observed in the submillisecond time domains in the A2/TEA system is mainly due to the contribution of neutral hydrogenated radicals.

Photoreduction mechanism

Photoinduced electron transfer (PET) should generate a contact radical ion pair, CRIP, which can decay by the following three pathways: (1) back electron transfer within the CRIP, (2) diffusional transformation of the CRIP to a solvent-separated radical ion pair, SSRIP and (3) proton transfer from the radical cation of the amine (not possible for non-H-donating amines TMP or DABCO) to the radical anion of the substrate, forming a geminate radical pair, GRP, [AH$^{\bullet}$ ••• R$_2$NC$^{\bullet}$HR′]. The solvent-separated radical ion pair, formed in acetonitrile and involving DABCO likely lacks spin correlation and decays by back electron transfer with a rate constant $k_{-ET} \approx 5 \times 10^4$ s^{-1} for both AOIA A1 and A2.

With TEA, an H-donating amine, the radical ion pair, [A$^{\bullet-}$ ••• TEA$^{\bullet+}$], has two main pathways of deactivation: (1) back electron transfer within the CRIP and/or (2) proton transfer from TEA$^{\bullet+}$ to A$^{\bullet-}$ leading to AN1H$^{\bullet}$ and AOH$^{\bullet}$, likely in equilibrium, eventually leading to metastable ions A1OH$^-$/A2OH$^-$ after a second electron transfer from the reductive α-aminoalkyl radical to the respective hydrogenated radicals within the GRP. The presence of these metastable anions A1OH$^-$/A2OH$^-$ is the only way to explain the C4 and C6 H/D isotopic exchange observed for the AOIA and aromatic OIA (20).

CONCLUSIONS

Spectral and kinetic data regarding the triplets, radical anions/radical ion pairs and neutral hydrogenated radicals derived from two A, that is 7*H*-benzo[*e*]perimidin-7-one (3-AOIA, A1) and its 2-methyl derivative (2-Me-3-AOIA, A2) are reported. The second N-atom (N3) in the ring containing N1-atom affects the triplet energies (E^T), which were found to be more than 10 kJ mol^{-1} less than the E^T measured for triplet states derived from oxoisoaporphines (^{3}OIA and ^{3}5-MeO-OIA) (24). On the other hand, methyl substitution at C2-atom in 2-Me-3-AOIA does not change the triplet energy in comparison to 3-AOIA. However, it affects the proton transfer rate constant (k_{H+}), which was found to be 2.9–5-fold larger for 2-Me-3-AOIA.

Formation of two neutral hydrogenated radicals, AN1H$^{\bullet}$ and AOH$^{\bullet}$, was confirmed experimentally by LFP and PR. These radicals likely exist in equilibrium. One of them, AOH$^{\bullet}$, undergoes transformation by a second electron transfer to the metastable photoproduct AOH$^-$, which accounts for the H/D isotopic exchange previously reported (20).

Acknowledgements—We thank E.S.S. for the azaoxoisoaporphines samples. C.A. thanks CONICYT for the Ph.D. fellowship, Project No. 24091001 and the final Fellowship to write the Doctoral Thesis. Thanks are also due to Universidad de Chile for the research stay fellowship accomplished in the Institute of Nuclear Chemistry and Technology, Warsaw, Poland. J.R.F thanks FONDECYT grants Nos. 1070623, 1100121 & 7080096 for the financial support. We thank Dr. Gordon L. Hug for his careful reading of the manuscript.

REFERENCES

1. Killmer, L., F. G. Vogt, A. J. Freyer, M. D. Menachery and C. M. Adelman (2003) Lakshminine, a new rare oxoisoaporphine alkaloid from Sciadotenia toxifera, and structural revisions of telazoline and teladiazoline, two related oxoaporphines from Telitoxicum peruvianum and T-glaziovii. *J. Nat. Prod.* **66**, 115–118.
2. Sugimoto, Y., H. A. A. Babiker, S. Inanaga, M. Kato and A. Isogai (1999) Oxoisoaporphines from Menispermum dauricum. *Phytochemistry* **52**, 1431–1435.
3. Yu, B. W., L. H. Meng, J. Y. Chen, T. X. Zhou, K. F. Cheng, J. Ding and G. W. Qin (2001) Cytotoxic oxoisoaporphine alkaloids from Menispermum dauricum. *J. Nat. Prod.* **64**, 968–970.
4. Flors, C. and S. Nonell (2006) Light and singlet oxygen in plant defense against pathogens: Phototoxic phenalenone phytoalexins. *Accounts. Chem. Res.* **39**, 293–300.
5. Flors, C., P. R. Ogilby, J. G. Luis, T. A. Grillo, L. R. Izquierdo, P. L. Gentili, L. Bussotti and S. Nonell (2006) Phototoxic phytoalexins. Processes that compete with the photosensitized production of singlet oxygen by 9-phenylphenalenones. *Photochem. Photobiol.* **82**, 95–103.
6. Schmidt, R., C. Tanielian, R. Dunsbach and C. Wolff (1994) Phenalenone, a universal reference compound for the determination of quantum yields of singlet oxygen $O_2(^1\Delta_g)$ sensitization. *J. Photoch. Photobio. A* **79**, 11–17.
7. Martí, C., O. Jürgens, O. Cuenca, M. Casals and S. Nonell (1996) Aromatic ketones as standards for singlet molecular oxygen $O_2(^1\Delta_g)$ photosensitization. Time-resolved photoacoustic and near-IR emission studies. *J. Photoch. Photobio. A* **97**, 11–18.
8. Lazzaro, A., M. Corominas, C. Marti, C. Flors, L. R. Izquierdo, T. A. Grillo, J. G. Luis and S. Nonell (2004) Light- and singlet oxygen-mediated antifungal activity of phenylphenalenone phytoalexins. *Photoch. Photobio. Sci.* **3**, 706–710.
9. Flors, C., C. Prat, R. Suau, F. Najera and S. Nonell (2005) Photochemistry of phytoalexins containing phenalenone-like chromophores: Photophysics and singlet oxygen photosensitizing properties of the plant oxoaporphine alkaloid oxoglaucine. *Photochem. Photobiol.* **81**, 120–124.
10. Castro-Castillo, V., M. Rebolledo-Fuentes, C. Theoduloz and B. K. Cassels (2010) Synthesis of lakshminine and antiproliferative testing of related oxoisoaporphines. *J. Nat. Prod.* **73**, 1951–1953.
11. Castro-Castillo, V., C. Suarez-Rozas, A. Pabon, E. G. Perez, B. K. Cassels and S. Blair (2013) Synthesis and antiplasmodial activity of some 1-azabenzanthrone derivatives. *Bioorgan. Med. Chem. Lett.* **23**, 327–329.
12. Prado-Prado, F., X. Garcia-Mera, M. Escobar, E. Sobarzo-Sanchez, M. Yanez, P. Riera-Fernandez and H. Gonzalez-Diaz (2011) 2D MI-DRAGON: A new predictor for protein-ligands interactions and theoretic-experimental studies of US FDA drug-target network, oxoisoaporphine inhibitors for MAO-A and human parasite proteins. *Eur. J. Med. Chem.* **46**, 5838–5851.
13. Dzieduszycka, M., S. Martelli, M. Arciemiuk, M. M. Bontemps-Gracz, A. Kupiec and E. Borowski (2002) Effect of modification of 6-[(Aminoalkyl)amino]-7H-benzo[e]-perimidin-7-ones on their cytotoxic activity toward sensitive and multidrug resistant tumor cell lines. Synthesis and biological evaluation. *Bioorgan. Med. Chem.* **10**, 1025–1035.
14. Bu, X., J. Chen, L. W. Deady, C. L. Smith, B. C. Baguley, D. Greenhalgh, S. Yang and W. A. Denny (2005) Synthesis and cytotoxic activity of N-[(alkylamino)alkyl]carboxamide derivatives of 7-oxo-7H-benz[de]anthracene, 7-oxo-7H-naphtho[1,2,3-de]quinoline, and 7-oxo-7H-benzo[e]perimidine. *Bioorgan. Med. Chem.* **13**, 3657–3665.

15. Stefanska, B., M. Dzieduszycka, S. Martelli, J. Tarasiuk, M. Bontempsgracz and E. Borowski (1993) 6-[(Aminoalkyl)Amino]-substituted 7H-benzo[E]perimidin-7-ones as novel antineoplastic agents – Synthesis and biological evaluation. *J. Med. Chem.* **36**, 38–41.
16. Stefanska, B., M. Dzieduszycka, M. M. Bontemps-Gracz, E. Borowski, S. Martelli, R. Supino, G. Pratesi, M. De Cesare, F. Zunino, H. Kusnierczyk and C. Radzikowski (1999) 8,11-dihydroxy-6-[(aminoalkyl)amino]-7H-benzo[e]perimidin-7-ones with activity in multidrug-resistant cell lines: Synthesis and antitumor evaluation. *J. Med. Chem.* **42**, 3494–3501.
17. Borovlev, I. V., O. P. Demidov, A. V. Aksenov and A. F. Pozharskii (2004) Heterocyclic analogs of pleiadiene: LXXIV. peri-cyclizations in the perimidine series. Synthesis of 1,3-diazapyrene derivatives. *Russ. J. Org. Chem+*. **40**, 895–901.
18. Tang, H., X. D. Wang, Y. B. Wei, S. L. Huang, Z. S. Huang, J. H. Tan, L. K. An, J. Y. Wu, A. S. C. Chan and L. Q. Gu (2008) Oxoisoaporphine alkaloid derivatives: Synthesis, DNA binding affinity and cytotoxicity. *Eur. J. Med. Chem.* **43**, 973–980.
19. Tang, H., F.-X. Ning, Y.-B. Wei, S.-L. Huang, Z.-S. Huang, A. S.-C. Chan and L.-Q. Gu (2007) Derivatives of oxoisoaporphine alkaloids: A novel class of selective acetylcholinesterase inhibitors. *Bioorg. Med. Chem. Lett.* **17**, 3765–3768.
20. Aliaga, C., M. Cerón-Neculpán, C. Saitz, C. Jullian, E. Sobarzo-Sánchez and J. R. De la Fuente (2011) Oxoisoaporphines: Regioselective deuterium labelling involving the metastable hydrogenated photoproduct anions. *J. Photoch. Photobio. A* **222**, 360–365.
21. De la Fuente, J. R., C. Jullian, C. Saitz, V. Neira, O. Poblete and E. Sobarzo-Sanchez (2005) Unexpected formation of 1-diethylaminobutadiene in photosensitized oxidation of triethylamine induced by 2,3-dihydro-oxoisoaporphine dyes. A H^1 NMR and isotopic exchange study. *J. Org. Chem.* **70**, 8712–8716.
22. De la Fuente, J. R., V. Neira, C. Saitz, C. Jullian and E. Sobarzo-Sanchez (2005) Photoreduction of oxoisoaporphine dyes by amines: Transient-absorption and semiempirical quantum-chemical studies. *J. Phys. Chem. A* **109**, 5897–5904.
23. De la Fuente, J. R., C. Jullian, C. Saitz, E. Sobarzo-Sanchez, V. Neira, C. Gonzalez, R. Lopez and H. Pessoa-Mahana (2004) Photoreduction of oxoisoaporphines. Another example of a formal hydride-transfer mechanism. *Photoch. Photobio. Sci.* **3**, 194–199.
24. De la Fuente, J. R., C. Aliaga, C. Poblete, G. Zapata, C. Jullian, C. Saitz, A. Cañete, G. Kciuk, E. Sobarzo-Sanchez and K. Bobrowski (2009) Photoreduction of oxoisoaporphines by amines: Laser flash and steady-state photolysis, pulse radiolysis, and TD-DFT studies. *J. Phys. Chem. A*, **113**, 7737–7747.
25. Bu, X., L. W. Deady, G. J. Finlay, B. C. Baguley and W. A. Denny (2001) Synthesis and cytotoxic activity of 7-oxo-7H-dibenz [f, ij]isoquinoline and 7-Oxo-7H-benzo[e]perimidine derivatives. *J. Med. Chem.* **44**, 2004–2014.
26. De la Fuente, J. R., G. Kciuk, E. Sobarzo-Sanchez and K. Bobrowski (2008) Transient phenomena in the pulse radiolysis of oxoisoaporphine derivatives in acetonitrile. *J. Phys. Chem. A* **112**, 10168–10177.
27. De la Fuente, J. R., E. Sobarzo-Sanchez and K. Bobrowski (2006) Spectroscopic Characterization of Radical Species from 2,3 dihydro-oxoisoaporphines Generated by Flash Photolysis and Pulse Radiolysis. Proceedings of the 18th Conference on Physical Organic Chemistry, Warsaw University, Poland.
28. De la Fuente, J. R., A. Cañete, C. Saitz and C. Jullian (2002) Photoreduction of 3-phenylquinoxalin-2-ones by amines: Transient-absorption and semiempirical quantum-chemical studies. *J. Phys. Chem. A* **106**, 7113–7120.
29. Viteri, G., A. M. Edwards, J. De la Fuente and E. Silva (2003) Study of the interaction between triplet riboflavin and the α-, β(H)- and β(L)-crystallins of the eye lens. *Photochem. Photobiol.* **77**, 535–540.
30. Mirkowski, J., P. Wisniowski and K. Bobrowski (2001) In *INCT Annual Report 2000*, (Edited by INCT), pp. 31–33. INCT, Warsaw.
31. Bobrowski, K. (2005) Free radicals in chemistry, biology, and medicine: contribution of radiation chemistry. *Nukleonika* **50**(Suppl 3), S67–S76.
32. Bobrowski, K., G. Dzierzkowska, J. Grodkowski, Z. Stuglik, Z. P. Zagorski and W. L. McLaughlin (1985) A pulse radiolysis study of the leucocyanide of malachite green dye in organic solvents. *J. Phys. Chem.* **89**, 4358–4366.
33. Boule, P. and J. F. Pilichowski (1993) Comments about the use of aberchrome (Tm)-540 in chemical actinometry. *J. Photoch. Photobio. A* **71**, 51–53.
34. Reichardt, C. (1990) *Solvents and Solvent Effects in Organic Chemistry*. VCH, New York.
35. Sobarzo-Sánchez, E., P. G. Soto, C. Valdés Rivera, G. Sánchez and M. E. Hidalgo (2012) Applied biological and physicochemical activity of isoquinoline alkaloids: Oxoisoaporphine and boldine. *Molecules* **17**, 10958–10970.
36. Sobarzo-Sánchez, E. and E. U. Villares (2011) Patent ES 2357926 Type A1. Preparation of nitrogen based heterocycles for the production of oxygen singlets.. Universidad de Santiago de Compostela, Spain.
37. Murov, S. L., I. Carmichael and G. L. Hug (1993) *Handbook of Photochemistry*. Dekker, New York.
38. Brede, O., D. Beckert, C. Windolph and H. A. Gottinger (1998) One-electron oxidation of sterically hindered amines to nitroxyl radicals: Intermediate amine radical cations, aminyl, alpha-aminoalkyl, and aminylperoxyl radicals. *J. Phys. Chem. A* **102**, 1457–1464.